

Single-mode fibre coupler with the 3-dB splitting ratio simultaneously at 0.83 and 1.3 μm

V.M. Gelikonov, G.V. Gelikonov

Abstract. The problem of designing a two-wave single-mode-fibre 3-dB coupler is considered. The method is proposed for adjusting the parameters of the coupler for simultaneous use of radiation at 0.83 and 1.3 μm in one fibre interferometer. The dependence of the coupling efficiency on the wavelength is studied experimentally for different angle mismatches of fibres in the coupler. The results of experiments and numerical calculations are presented.

Keywords: optical two-wave coupler, single-mode fibre, fibre interferometer.

1. Introduction

The development of a single-mode fibre directional coupler (2×2) with the 3-dB splitting of optical radiation simultaneously at wavelengths of 0.83 and 1.3 μm is of interest for some problems of applied fibre optics [1–4]. The spectral properties of a symmetrical 3-dB polished coupler provide the equal splitting of optical radiation simultaneously at several certain wavelengths; however, an arbitrary choice of two wavelengths is impossible. The wavelength dependence of the coupling efficiency in symmetric fibre couplers is commonly used for multiplexing–demultiplexing of radiation at different wave-lengths. At certain, substantially different wavelengths (0.64 and 1.3 μm) an almost complete power transfer at the longer wavelength and a sufficiently weak power transfer at the shorter wavelength can be realised [5]. The close wavelengths (in the range from 1.3 to 1.65 μm) can be separated by using single power transfer at the shorter wavelength and double transfer at the longer wavelength [6]. It was shown in [6] that demultiplexing with a small mutual penetration is possible only when single and double coupling lengths of two fibres at the corresponding wavelengths are identical.

The two-wave splitting of optical powers in certain identical proportions was performed in planar couplers [7–9] for more close wavelengths (1.3 and 1.55 μm) by increasing the coupler pass band. The wavelength dependen-

ces of the coupling efficiency were levelled in these papers by fabricating asymmetric planar waveguide structures.

The spectral properties of spliced tapered single-mode X-couplers can be controlled in a sufficiently broad range by changing the geometry of a splicing region. Thus, the authors of [10] studied, in particular, the possibility of obtaining an extremely high spectral sensitivity (radiation splitting with the selectivity $\Delta\lambda \leq 0.6$ nm) by selecting appropriately the coupling coefficient and the length of a fibre segment on which optical coupling is performed. One of the approaches to the development of broadband spliced couplers is described in [11]. The maximum bandwidth was achieved when the cross section of the splicing region was dumbbell-like, with the aspect ratio of 1.8.

While solving a number of applied fibreoptic problems, which impose strict requirements on the splitting ratio of polarisation modes, the best results can be obtained by using polished couplers. It is known from the literature that the spectral properties of single-mode polished fibre couplers can be controlled by violating the symmetry in the wave-transfer region. Unlike planar couplers, the structure asymmetry in polished couplers is commonly used to narrow down the spectral region of interaction. Thus, asymmetric polished single-mode couplers were used for the development of narrow-band multiplexers (demultiplexers) [12].

The required asymmetry was achieved by using fibres of different diameters and different refractive indices of the core, and also due to the inequality of the residual layers of silica claddings of the fibres. For symmetry of this type, however, it is impossible to equalise the coupling efficiencies simultaneously at two quite separated wavelengths because the equality of the phase velocities in both fibres is achieved only at a certain wavelength.

Although numerous methods for controlling the spectral properties of couplers have been described in the literature available to us, the possibility of using an additional degree of freedom, namely, the angular mismatch of optically coupled fibres has not been discussed so far. In this paper, we propose a new method for equalising the coupling efficiencies simultaneously at two strongly separated wavelengths in a symmetric fibre coupler, which is based on the use of the angular mismatch between fibre cores.

2. Effect of the angular mismatch

As mentioned above, it is necessary to use two radiation sources emitting at 0.83 and 1.3 μm in one fibre interferometer in some applications. In fibres with a rather small core diameter and a great difference between the refractive

V.M. Gelikonov, G.V. Gelikonov Institute of Applied Physics, Russian Academy of Sciences, ul. Ul'yanova 46, 603950 Nizhnii Novgorod, Russia; e-mail: grig@ufp.appl.sci-nnov.ru

indices of the core and cladding, which are used in sensors, radiation with a simplest structure can propagate at both these wavelengths (of course, when the level of losses in the fibre is small). However, light losses in a particular interferometer at a longer wavelength at fibre bends can be in this case quite high and virtually unavoidable. For this reason, to obtain the maximum signal-to-noise ratio for an interferometric signal, all the parameters of the interferometer should be optimised. In particular, it is desirable to obtain the 3-dB splitting ratio simultaneously for both wavelengths. As a rule, this condition is not fulfilled for an arbitrary coupler.

Figure 1 shows the dependences of the efficiency of radiation coupling $K_{14} = P_{14}/(P_{12} + P_{14})$ to the adjacent fibre on the distance h_0 between the centres of fibres for a coupler based on a P-63 experimental fibre (Fibertek, Arzamas, Russia) with the core diameter $2a = 3.77 \mu\text{m}$ and the refractive index difference $\Delta n = 0.008$ (the cutoff wavelength is $0.75 \mu\text{m}$) at the radius of curvature of grooves equal to 30 cm, which were calculated using expressions presented in [12]. In this fibre, single-mode radiation propagates at both wavelengths with relatively low additional losses at $1.3 \mu\text{m}$ when the fibre is bent. Here, P_{12} is the optical power propagated through the coupler over the initial fibre and P_{14} is the power coupled to the adjacent fibre. The thickness of the intermediate immersion layer with the refractive index $n = 1.445$ was $0.1 \mu\text{m}$.

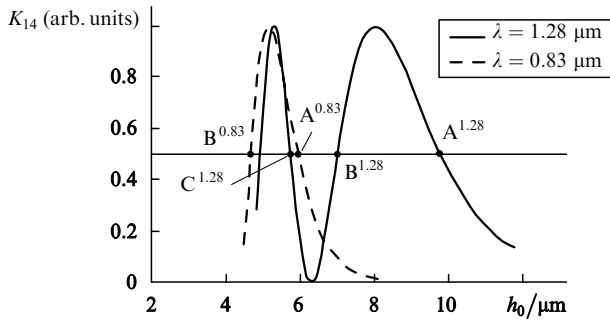


Figure 1. Dependences of the coupling coefficient K_{14} on the distance h_0 between fibre centres for the $0.1\text{-}\mu\text{m}$ thick immersion layer. Points $A^{1.28}$, $B^{1.28}$, and $C^{1.28}$ indicate the distances h_0 between fibre centres ($z = 0$) at which half-splitting of the optical power between fibres is performed at $1.28 \mu\text{m}$; points $A^{0.83}$ and $B^{0.83}$ indicate the same for a wavelength of $0.83 \mu\text{m}$ ($h_0 = d_1 + d_2 + 2a = h_1 + h_2$). The parameter $c_0 L$ at points A, B, C is $\pi/4$, $3\pi/4$, $5\pi/4$, respectively, where c_0 is the coupling parameter, L is the length at which coupling is performed. The angle α and lateral displacement are equal to zero.

As follows from Fig. 1, whatever the distance between the centres of fibres, the 3-dB splitting ratio is not achieved simultaneously at both wavelengths. To simplify the consideration, we will use the expressions for the distribution of radiation power, initially coupled to one of the fibres, at the outputs of the coupler for two identical weakly coupled fibres without an immersion layer between two equal parts (halves) of the coupler [13]:

$$P_{12} = P_0 \cos^2(c_0 L), \quad P_{14} = P_0 \sin^2(c_0 L), \quad (1)$$

where

$$c_0 L_{\text{eff}} = \int_{-\infty}^{+\infty} c(z) dz; \quad (2)$$

P_0 is the power incident on the input of coupler 1; $c(z)$ is the local coupling coefficient for two coupled modes upon removing from the central transfer region in the longitudinal direction by the value z (Fig. 2); L_{eff} is the effective interaction length of the optical modes of the coupler; and c_0 is the coupling coefficient at the centre of the interaction region for $z = 0$.

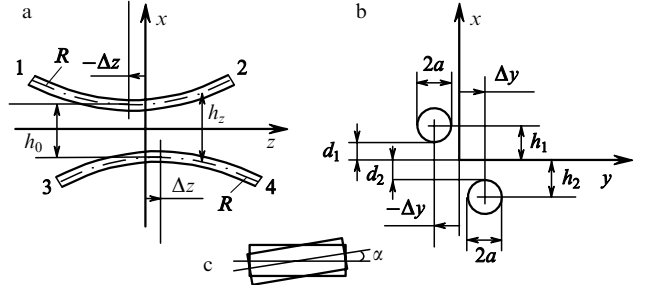


Figure 2. Scheme of the coupler: side view (a), perpendicular cross section ($z = 0$) at the centre of the region of mode coupling (b), and the view of two parts of the coupler oriented at an angle α to each other (c). The numbers 1–4 indicate the inputs and outputs of the coupler.

Consider the effect of additional degrees of freedom. In a symmetric coupler consisting of two identical parts, the strength of local coupling of optical modes of fibres depends [12] on the initial distance h_0 between the core centres and the coordinate z , i.e., $h_i = d_i + a_i + z^2/2R$, where R is the radius of curvature of a groove in which the fibre is placed. Let us introduce into this dependence the longitudinal displacement Δz of each of the parts of the coupler and the lateral displacement Δy of grooves, as was done in [13], and the angle α between the grooves

$$h_1(z) = \left\{ \left[d_1 + a + \frac{(z + \Delta z)^2}{2R} \right]^2 + \left(\Delta y + z \tan \frac{\alpha}{2} \right)^2 \right\}^{1/2}, \quad (3)$$

$$h_2(z) = \left\{ \left[d_2 + a + \frac{(z - \Delta z)^2}{2R} \right]^2 + \left(-\Delta y - z \tan \frac{\alpha}{2} \right)^2 \right\}^{1/2}.$$

The parameters $d_{1,2}$, Δz , Δy , and α determine the strength of optical coupling between the fibres. One can see from expression (3) that the presence of only longitudinal displacement Δz is equivalent to the increase in the thickness of the total residual layer $d = d_1 + d_2$. The effect of the lateral displacement Δy on the coupling strength was calculated and experimentally studied in [13]. It follows from [13] that the longitudinal displacement $2\Delta z$ between the regions of maximum power transfer and the lateral displacement $2\Delta y$ are equivalent to the increase in the residual-layer thickness d . The sensitivity to the displacement from the optimal adjustment for $\alpha = 0$ is h_0/R times lower in the direction z than in the direction y .

It was also shown in [13] that the minimal distance h_0 determines the coupling coefficient c_0 between fibres, while the curvature of the fibre bending in grooves controls the effective interaction length L_{eff} of the modes. It is obvious that the parallel displacements of the parts of the coupler along z and y can lead only to the parallel displacement of dependences in Fig. 1 along the abscissa, but they cannot draw together the half-splitting points for wavelengths 0.83 and $1.28 \mu\text{m}$. To verify this statement using expressions for

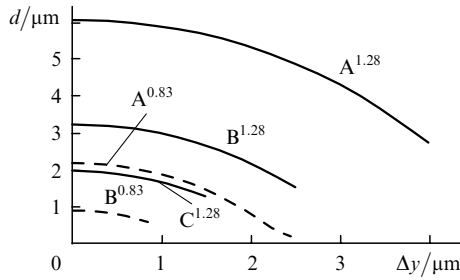


Figure 3. Dependences of the distance d along the vertical between fibre cores in the case of half-splitting on the lateral displacement Δy between fibres for $\lambda = 0.83 \mu\text{m}$ for single and double power transfers (dashed curves) and for single, double, and triple power transfers (solid curves). The immersion layer thickness is $0.1 \mu\text{m}$, the angle $\alpha = 0$.

[12], we calculated the dependences of the values of d at the half-splitting points $A^{1.28}$, $B^{1.28}$, $C^{1.28}$, $A^{0.83}$, and $B^{0.83}$, presented in Fig. 3, on the lateral displacement Δy between the fibres.

As follows from Fig. 3, the parallel displacements along the y axis (and also along the z axis) do not give the desirable result. Therefore, the lateral displacement cannot provide the 3-dB splitting ratio simultaneously at 0.83 and $1.28 \mu\text{m}$.

A substantially different is the character of the angular mismatch α . The presence of the angle α is equivalent to the decrease in the radius of curvature R . In this case for $\Delta z = 0$ and $\Delta y = 0$, the value of h is described by the expression

$$h \approx \left(d^2 + \frac{d + R \tan(\alpha/2)}{R} z^2 \right)^{1/2} = \left(d^2 + \frac{d}{R_{\text{eff}}} z^2 \right)^{1/2}. \quad (4)$$

Here, $R_{\text{eff}} = R[d/(d + R \tan^2 \alpha/2)]$. The effective radius of curvature of the fibre bending decreases by half when $\alpha_{0.5} = 2 \arctan[(d/R)^{1/2}]$. Thus, for $d = 5.5 \mu\text{m}$ and $R = 0.3 \text{ m}$, we have $R_{\text{eff}} = R/2$ for $\alpha_{0.5} = 0.5^\circ$.

In the case of parabolic approximation $z^2 \ll h_0 R$, the effective interaction length is [13]

$$L_{\text{eff}} = \left(\frac{\pi R_{\text{eff}} a}{v} \right)^{1/2}, \quad (5)$$

where a is the fibre radius; v is the transverse parameter of the mode outside the fibre core, which determines the dependence of L_{eff} on the wavelength. One can see that the ratio of the effective interaction lengths for the two wavelengths in this model is independent of the angle between the fibre cores.

The introduction of the angle α also affects the local coupling coefficient $c = c(z)$. According to [13], by neglecting an immersion layer between the parts of the coupler and assuming that $\Delta n/n = (n_1 - n_2)/n_1 \ll 1$, the coefficient c is expressed in terms of the modified Hankel functions

$$c = \frac{\lambda}{2\pi n_1} \frac{u^2}{a^2 V^2} \frac{K_0(vh/a)}{K_1^2(v)}. \quad (6)$$

As the angle increases, the effective radius R_{eff} of fibre curvature and the local coupling coefficient $c(z)$ decrease. In this case, the condition $c_0 L = \pi/4, 3\pi/4, 5\pi/4$ will be satisfied at smaller distances h_0 between fibre cores. Because the derivative dc/dh increases with decreasing h , the effect

of the angle α on the integrated coupling coefficient c successively increases on passing from points A to points B and C. For a P-63 fibre, the transverse parameter v of the mode outside the core at wavelengths 0.83 and $1.28 \mu\text{m}$ is 0.617 and 1.16 , respectively. In this case, the argument vh/a of the function K_0 in expression (6) for points $A^{0.83}$ and $B^{1.28}$ (Fig. 1) is 1.35 and 1.08 , respectively. It is obvious that the half-splitting point $B^{1.28}$ will shift with increasing angle α to lower values of h by a greater value compared to the point $A^{0.83}$, because the corresponding value of the function K_0 at $1.28 \mu\text{m}$ has a smaller argument. This angular dependence is preserved for real values of L_{eff} and also for nonzero Δz and Δy .

Figure 4 shows the dependences of d on the angle α (for $z = 0$) for the P-63 fibre coupler at $0.83 \mu\text{m}$ at points A, B and at $1.28 \mu\text{m}$ at points A, B, C. Each value of d on these curves corresponds to the equal splitting of optical powers in the coupler (at the corresponding wavelengths). The dependences were calculated using expressions from [12] in the presence of the immersion layer between fibres in the case of total internal reflection at the glass-immersion layer interface.

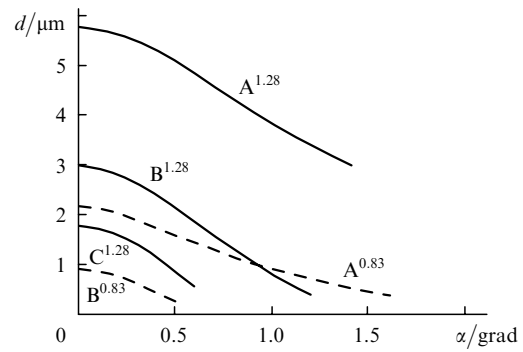


Figure 4. Dependences of the distance d along the vertical between fibre cores in the case of half-splitting on the angle α for $\lambda = 0.83 \mu\text{m}$ for single and double power transfers (dashed curves) and for $\lambda = 1.28 \mu\text{m}$ for single, double, and triple power transfers (solid curves). The immersion-layer thickness is $0.1 \mu\text{m}$.

As follows from Fig. 4, for $\alpha = 0.9^\circ$, the curves $A^{0.83}$ and $B^{1.28}$ are intersected (at $d = 1.05 \mu\text{m}$). The presence of such an intersection means that the half-splitting (3-dB) of the optical power can be performed between the fibres simultaneously at 0.83 and $1.28 \mu\text{m}$.

Figure 5 shows the spectral dependences of the coefficient K_{14} of optical power transfer to the mode of an adjacent fibre for $d = 1.05 \mu\text{m}$ and $= 0.9^\circ$ (i.e., for the found conditions of simultaneous 3-dB coupling at 0.83 and $1.28 \mu\text{m}$) and also for $\alpha = 0$ and the same d . Comparison of these dependences shows that the curve obtained for $\alpha = 0.9^\circ$ corresponds to a more broadband coupler under the condition of an exact 3-dB coupling level at 0.83 and $1.28 \mu\text{m}$.

3. Experimental results

Consider the results of the experimental study of spectral parameters of the 3-dB two-wave coupler whose parts were made of P-63 fibres with slightly different core diameters (3.77 and $3.6 \mu\text{m}$). To preserve the condition of total internal reflection, the parts of the coupler superimposed

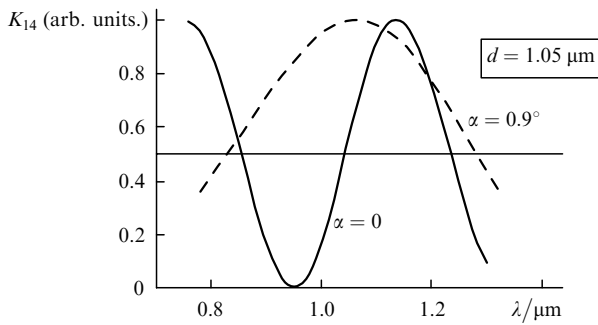


Figure 5. Spectral dependences of the coefficient K_{14} of optical-power coupling to the mode of an adjacent fibre for different α .

via the immersion liquid with the refractive index lower than that of silica. The fibre cores could be oriented parallel to each other or at a certain angle with the help of precision mechanical positioners. Radiation from an incandescent lamp passed through a ZMR-3 mirror monochromator and was incident on the input 1 of the fibre coupler. The radiation wavelength was varied from 0.7 to 1.4 μm . The powers P_{12} and P_{14} at outputs 2 and 4 were measured (Fig. 2).

Figure 6 shows the experimental dependences of $K_{14} = P_{14}/(P_{12} + P_{14})$ on the wavelength for three specified angles α . These curves were obtained by adjusting the coupler to the 3-dB coupling level at 0.83 μm . The dashed curve in Fig. 6 shows the wavelength dependence of K_{14} calculated for $\alpha = 0.9^\circ$ taking into account that the parameters of fibres in different parts of the coupler were different. It follows from Fig. 6 that for $\alpha = 0$ the relative values K_{14} of the coupled power do not achieve their limiting values (i.e., zero and unity). This is explained by the different optical parameters of modes in fibres, namely, by different fibre core diameters [14, 15].

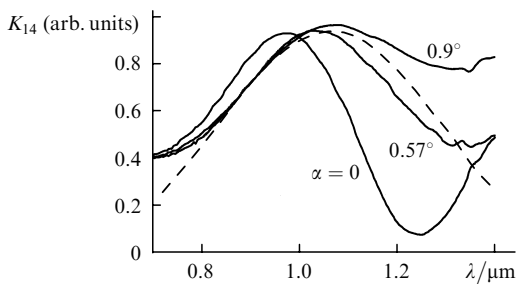


Figure 6. Spectral experimental dependences of K_{14} for different α . The dashed curve is the calculation for $\alpha = 0.9^\circ$.

For wavelengths shorter than the cutoff wavelength (0.75 μm), the experimental curves deviate from the calculated one, which can be explained by the influence of higher-order modes. As follows from the experimental data presented above, the introduction of the angular mismatch between fibres broadens the pass band of the coupler and provides the 3-dB coupling at the two chosen wavelengths. However, the influence of the angular mismatch observed in experiments was greater than that predicted by calculations. Because the surface of the parts of the coupler was non-planar, the thickness of the immersion layer slightly increased with removing from the centre. We assume that this effect can be explained by the influence of the

inhomogeneity of the immersion-layer thickness, which can reduce R_{eff} .

4. Conclusions

We have shown that the introduction of the angular mismatch between fibres in addition to other degrees of freedom substantially expands the possibilities of the optical adjustment of a symmetric single-mode polished coupler and provides a more flexible control of its spectral parameters. In particular, this resulted in the increase in pass band of the coupler and provided the 3-dB radiation coupling at 0.83 and 1.28 μm . The results used in this paper have been published in [16].

Acknowledgements. The authors thank D.V. Shabanov for the adjustment of spectral instruments. This work was partially supported by the Russian Foundation for Basic Research (Grant Nos 99-02-16265 and 00-15-96732).

References

1. Gelikonov G.V., Gelikonov V.M., et al., in *Dig. Conf. Laser and Electro-Optics* (Washington, DC, Baltimore: Optical Society of America, 1997) Vol.11, p.210.
2. Roper S.N., Moores M.D., Gelikonov G.V., et al. *J. Neurosci. Methods*, **80**, 91 (1998).
3. Feldchtein F.I., Gelikonov G.V., Gelikonov V.M., Iksanov R.R., Kuranov R.V., Sergeev A.M., Gladkova N.D., Ourutina M.N., Warren J.A. Jr., Reitze D.H. *Opt. Express*, **3**, 239 (1998).
4. Gelikonov V.M., Gelikonov G.V., Dolin L.S., Kamensky V.A., Sergeev A.M., Shakhova N.M., Gladkova N.D., Zagaynova E.V. *Laser Phys.*, **13**, 692 (2003).
5. Gelikonov V.M., Gelikonov G.V., Shabanov D.V. *Opt. Zh.*, **67**, 81 (2000).
6. Januar I., Mickelson A.R. *Opt. Lett.*, **18**, 417 (1993).
7. Takagi A., Jinguji K., Kawachi M. *Electron. Lett.*, **26**, 132 (1990).
8. Takagi A., Jinguji K., Kawachi M. *IEEE J. Quantum Electron.*, **28**, 848 (1992).
9. Takagi A., Jinguji K., Kawachi M. *J. Lightwave Techn.*, **10**, 735 (1992).
10. Bulushev A.G., Gurov Y.V., Dianov E.M., Okhotnikov O.G., Prokhorov A.M., Shurukhin B.P. *Opt. Lett.*, **13**, 230 (1988).
11. Xue-Heng Z. *Electron. Lett.*, **24**, 1018 (1988).
12. Zengerle R., Leminger O. *Opt. Quantum Electron.*, **18**, 365 (1986).
13. Digonnet M.J.F., Show H.J. *IEEE J. Quantum Electron.*, **18**, 746 (1982).
14. Unger H.-G. *Planar Optical Waveguides and Fibres* (Oxford: Clarendon Press, Oxford, 1977; Moscow: Mir, 1980).
15. Snyder A., Love D. *Optical Waveguide Theory* (London–New York: Chapman and Hall, 1983; Moscow: Radio i Svyaz', 1987).
16. Gelikonov V.M., Gerlikonov G.V. *Preprint of Inst. Appl., RAS*, (586) (Nizhnii Novgorod, 2001) p. 1.